Spray Assisted Layer-by-Layer Assembled One-Bilayer Polyelectrolyte Reverse Osmosis Membranes

Qiang Li,[a] George Q. Chen,[b] Liang Liu,[b] and Sandra E. Kentish*[b]

[a] The Institute of Seawater Desalination and Multipurpose Utilization, SOA (Tianjin), Tianjin 300192, China

[b] Department of Chemical Engineering, The University of Melbourne, VIC 3010, Australia

*Corresponding Author E-mail: sandraek@unimelb.edu.au (S. E. Kentish).

Abstract

A single-bilayer polyelectrolyte reverse osmosis membrane was fabricated by a spray assisted layer-by-layer assembly approach using a polysulfone ultrafiltration membrane as a substrate, polyethyleneimine (PEI) as an adhesion promoter, poly(allylamine hydrochloride) (PAH) and poly(sodium-4-styrene sulfonate) (PSS) as polycation and polyanion, glutaraldehyde as a crosslinker and Pluronic F127 amphiphilic triblock copolymer as a surface modifier. The resulting active layer is ultrathin (*ca.* 70 nm) and has a flat, dense and uncharged surface in neutral solution. The salt rejection and permeate flux of the membrane gradually increases from 92 % to 94 %, and 11 L/m^{2}h to 30 L/m^{2}h respectively for a 2 g/L NaCl feed solution as the operating pressure increased from 1.6 MPa to 4.0 MPa. Additionally, the membrane shows good separation performance stability and protein fouling resistance using bovine serum albumin as a foulant model. The glutaradehyde plays a key role in enhancing salt rejection by forming imine bonds within the PEI layer and the PEI/PAH interlayer. The Pluronic F127 surface modifier improves the permeate flux due to its hydrophilicity and the resulting induced swelling providing channels for water flow. Further, the "brush-like" structure of the hydrophilic polyethylene oxide moieties on the membrane surface improves fouling resistance.

1. Introduction

The scarcity of fresh water is an increasingly serious global issue, due to population expansion, climate change, and environmental pollution [1,2]. To increase global fresh water reserves, reverse osmosis (RO) desalination is increasingly employed owing to its low energy consumption, low cost, and ease of operability [3,4]. While commercial RO membranes are formed by interfacial polymerization, layer-by-layer (LBL) assembly has emerged as a useful alternative approach [5,6] due to its simplicity and the use of aqueous solutions [7-9]. The process classically involves dipping the substrate in solutions of differently charged polyelectrolytes in turn, with intermediate rinsing steps. In comparison with the traditional interfacial polymerization approach, a wide range of molecules can be deposited *via* interlayer interactions such as electrostatics [10], hydrogen bonding [11], metal-ligand coordination [12] and covalent bonding [13]. The technique can provide precise control of hydrophilicity, surface charge and membrane thickness at the nanoscale.

LBL assembled membranes have mainly been developed for nanofiltration [14,15] and the approach has also been used in pervaporation, and forward osmosis [16,17]. These membranes usually have low NaCl rejection (< 80 %), due to poor membrane densification and the swelling of the polyelectrolytes in aqueous solution [18-20]. For example, Grooth *et al* [19] fabricated a 7-bilayer polyelectrolyte membrane by alternatively depositing poly(diallyldimethylammonium chloride) (PDADAMAC) and poly(sodium-4-styrene sulfonate) (PSS) on a sulfonated poly(ether sulfone) based ultrafiltration membrane using dipping. This membrane shows 71 % and 96 % rejection for 0.5 M NaCl and Na_2SO_4 aqueous solutions respectively. Covalent cross-linking between the deposited layers has been used to further increase the density of the membrane [21-23]. Park *et al* [21] reported an amide group crosslinked poly(allylamine hydrochloride) (PAH) / poly(acrylic acid) (PAA) polyelectrolyte membrane with 10 bilayers and 250 nm active-layer thickness

fabricated by dipping LBL assembly. This membrane exhibits high NaCl rejection (99.8 %) but low permeate flux (8 L/m^{2}h) under 2 MPa pressure for 2 g/L NaCl feed solutions.

The classical dipping LBL assembly approach usually take a few hours to several days to deposit sufficient bilayers to ensure a defect-free, dense structure [24,25]. Spray LBL assembly, as proposed by Schlenoff *et al* in 2000 [26] decreases the membrane fabrication time. This method can be used to spray polyelectrolytes onto any solvent-accessible two dimensional and/or three dimensional substrate [24,27]. For example, our group fabricated a glutaradehyde (GA) crosslinked polyelectrolyte RO membrane by spraying 10 bilayers of PAH and PSS onto a polysulfone (PSF) substrate [28]. The membrane possessed high NaCl rejection (90 %) for 2 g/L NaCl feed solution at 2.4 MPa operating pressure. However, it also showed low permeate flux (8 L/m^{2}h). This is because the high bilayer number, coupled with the glutaraldehyde crosslinking, resulted in a thick, dense membrane active layer. Further, the need for multiple bilayers still leads to a protracted manufacturing operation. The fabrication of a single bilayer RO membrane of comparable rejection but higher flux would facilitate production at a larger scale.

Surface modification using hydrophilic chemicals and/or nanostructured materials is a common strategy for optimizing the permeate flux and fouling resistance of water treatment membranes fabricated by interfacial polymerization and phase inversion approaches [29–31]. Pluronic F127 (PEO_{106}-PPO_{70}-PEO_{106}) is a triblock copolymer composed of two hydrophilic polyethylene oxide (PEO) chains surrounding a central hydrophobic polypropylene oxide (PPO) chain. It is often anchored onto the membrane surface to increase the hydrophilicity and fouling resistance [31-34]. The PEO segments can form “brush-like” structures on the surface after the polymer is swollen in aqueous solution [33]. For example, Falath *et al* fabricated a Pluronic F127 modified bisphenol A diglycidyl ether crosslinked Poly (vinyl alcohol) (PVA)/ gum Arabic RO membrane by a

dissolution casting solution method [34]. This research suggests that this modifier could be an effective way to optimize the hydrophilicity and separation performance of LBL membranes. However, to our knowledge, there have been no reports to date involving surface modification of LBL membranes using such a non charged polymer.

Herein we fabricate a GA crosslinked 1-bilayer polyelectrolyte membrane modified by Pluronic F127 *via* spray LBL assembly. A polysulfone ultrafiltration membrane is used as a substrate, PEI as an adhesion promoter, PAH and PSS as polycation and polyanion respectively. The salt rejection and permeate flux of this PEC membrane can reach up to 94 %, and 30 L/m^{2}h respectively under 4.0 MPa operating pressure for a 2 g/L NaCl aqueous solution. Importantly, the use of a single bilayer leads to a facile manufacturing technique that has great prospects for large-scale desalination operations.

2. Materials and Methods

2.1. Chemicals and materials

Branched polyethylenimine (PEI, Mw ~ 25,000), poly(sodium-4-styrene sulfonate) (PSS, Mw ~ 70,000), glutaraldehyde (GA, 25 wt% solution in water), Pluronic F127 (PEO_{106}–PPO_{70}–PEO_{106}, M_w ~ 12,600), and bovine serum albumin (BSA) were purchased from Sigma-Aldrich. Poly(allylamine hydrochloride) (PAH, Mw ~ 120,000 to 200,000) was obtained from Alfa Aesar. Sodium chloride, boric acid, potassium chloride, sodium hydroxide, and hydrochloric acid were purchased from Chem-Supply. The polysulfone (PSF) ultrafiltration substrate (MWCO ~ 92.5 kDa, A1) was kindly provided by GE Water. A commercial SW30 HR RO membrane was purchased from Dow Water and Process Solutions.

2.2. Polyelectrolyte membrane fabrication

To prepare a one-bilayer membrane, the PSF substrate (*ca.* 10×10 cm^2) was fixed to a hard plastic sheet which was held vertically. A gravity fed pressure spray gun (Austech Industries, Australia) was used to deliver each solution to the membrane. The gun reservoir was pressured with nitrogen at around 3.5 Bar to create a mist spray, with the distance between the substrate and nozzle of the sprayer around 20 cm. Initially, 8 ml of PEI aqueous solution (5 g/L) was sprayed as a primer layer. Then 8 ml of GA aqueous solution (0.1 mol/L) was sprayed as a cross linker. Subsequently, PSS aqueous solution (5 g/L), and PAH aqueous solution (5 g/L) were sequentially sprayed with the same volume to form one electrolyte bilayer. F127 aqueous solution (5 g/L) was sprayed onto the resulting membrane as a surface modifier. The final membrane (referred to as PEI/GA/PSS/PAH/F127) was dried in air at room temperature for at least 3 h to allow further crosslinking to occur. The time of each spraying step was 10 min. After each step except the GA spraying step, the substrate was rinsed by spraying purified water (MilliQ, Millipore) for 15 s to remove unabsorbed electrolytes.

To investigate the effect of the F127 modifier, membranes were also manufactured without this spray step (referred to as PEI/GA/PSS/PAH) as a control. An uncrosslinked membrane (referred to as PEI/PSS/PAH) was also fabricated as an additional control sample, where both the GA and F127 spray steps were omitted. Additionally, to explore the separation performance of the PEI primer layer, a membrane coated only with PEI and GA (referred to as PEI/GA) was fabricated.

.3. Surface property and structure characterization

The membrane surface functional groups were characterized using FTS 7000 Fourier transform infared (IR) spectrometer (Varian, USA) equipped with an attenuated total reflectance (ATR) accessory. A Surpass zeta potential analyser (Anton Paar, Austria) was employed to measure the surface charge properties using 1 mM potassium chloride aqueous solution as electrolyte. The membrane surface was also investigated using Quanta 200 F (FEI, USA) scanning electron microscopy (SEM) and the contact angle was obtained on an OCA 20 tensiometer (Dataphysics, USA) using purified water as a measurement solution.

2.4. Separation performance and stability evaluation

2 g/L of NaCl aqueous solution was used as feed solution to evaluate the rejection and permeate flux of the membranes using a crossflow rig consisting of three parallel CF042 cells (Sterlitech, USA) with *ca.* 42 cm^2 active membrane area under various testing pressure (1.6–4.0 MPa). Before collecting the permeate sample, all the membranes were compacted for 2 h under the test pressure. The salt rejection was calculated by conductivity measurement. The permeate flux was calculated based on the mass of permeate collected over time recorded by an Ohaus Pioneer balance. The separation performance of the commercial SW30 HR RO membrane was also evaluated using the same approach for comparison.

To evaluate the stability of the separation performance, the PEI/GA/PSS/PAH/F127 membrane was continuously tested for 32 h under 2.4 MPa pressure using 2 g/L NaCl feed solution by crossflow filtration as described above. The permeate was collected every 2 h for measuring the salt rejection and permeate flux.

152 To further investigate the desalination mechanism, the rejection of boron was also
153 determined *via* a dead-end filtration cell (Sterlitech HP4750) under 2.4 MPa pressure
154 respectively using *ca.* 20 mg/L boron aqueous solution with pH =4.0 and 11 as feed. Before
155 the rejection test, the membrane was compacted using purified water (MilliQ, Millipore)
156 under the same pressure for 2 h. The salt rejection was calculated by measuring the
157 concentrations of boron in the feed solution and permeate using Inductively Coupled
158 Plasma Optical Emission Spectrometry (Varian ICPOES 720 ES).

159 ***2.5. Fouling resistance evaluation***

160 1 g/L BSA aqueous solution was employed as a model foulant to evaluate the fouling
161 resistance of the membranes using the dead-end filtration cell mentioned above under 2.4
162 MPa operating pressure. In each cycle, the BSA solution was filtered for 8 h. The filtration
163 cell was then opened and the membrane flushed with purified water (MilliQ, Millipore) at
164 least 5 times (ca. 30 s each time). This cycle of fouling and cleaning was repeated three
165 times. Before the evaluation, the membrane was firstly compacted using purified water
166 under the same pressure for 2 h. The permeate was collected every 2 h to determine the
167 flux. The normalized permeate flux as indicated by the ratio of the flux (J) to the initial
168 flux (J_0) was utilized to evaluate the fouling resistance.

169

170 **3. Results and discussion**

171 ***3.1. Membrane surface properties***

172 The ATR-IR spectra (Fig. 1) show that the IR absorption signal of the PSF substrate is very
173 strong. The IR spectrum of the uncrosslinked PEI/PSS/PAH membrane (Fig. 1b) is nearly
174 identical to that of the PSF substrate (Fig. 1a). In contrast, the crosslinked

PEI/GA/PSS/PAH membrane (Fig. 1c) shows a broad peak at 3440 cm^{-1} attributed to the amine-group (N–H) stretching vibration of the deposited PAH and PEI. Another small peak at 1640 cm^{-1} can be assigned to the stretching of the imine (–C=N–) groups [28]. After Pluronic F127 is sprayed (Fig. 1d), the broad peak of the modified one-bilayer PEI/GA/PSS/PAH/F127 membrane at 3440 cm^{-1} becomes more well resolved due to the presence of the hydroxyl groups (O–H) of the F127 modifier on the membrane surface. Moreover, the peak related to the imine groups can be still observed in this membrane.

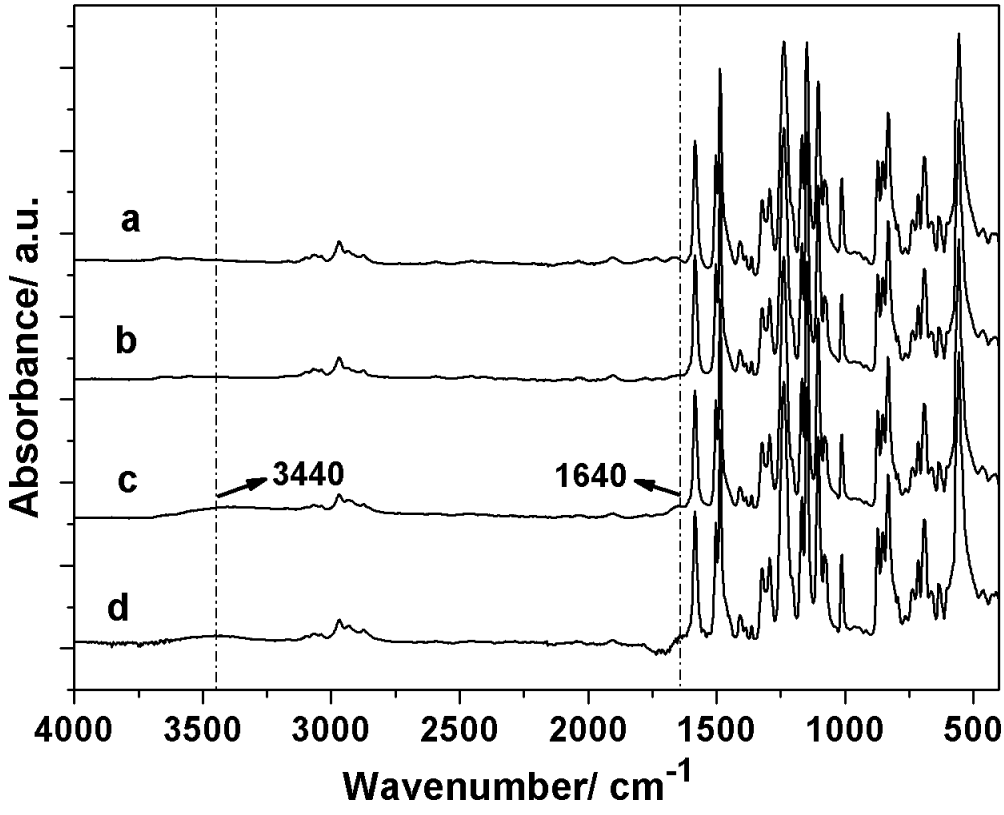

Fig. 1. ATR-IR spectra of (a) polysulfone substrate, (b) the uncrosslinked PEI/PSS/PAH membrane, (c) the crosslinked PEI/GA/PSS/PAH membrane, and (d) the F127 modified PEI/GA/PSS/PAH/F127 membrane.

These results indicate that there is very little polyelectrolyte absorbed on the substrate for the uncrosslinked PEI/PSS/PAH system (Fig. 1b). After GA is introduced during the membrane fabrication (PEI/GA/PSS/PAH), more PAH polyelectrolytes are anchored onto the substrate due to the formation of the imine bond (–C=N–) (Fig. 1c,d) between GA and the amine group containing polyelectrolytes (PEI and PAH).

From the zeta potential results (Fig. 2), it can be observed that after the polycation PEI was sprayed (Fig. 2a1), the substrate surface is positively charged in the whole of the pH measurement range (3.0–9.5). However, the addition of GA reduces the charge and an isoelectric point (IEP) appears at *ca.* pH 7.05 (Fig. 2a2). Subsequently, after the polyanion PSS was sprayed (PEI/GA/PSS), the substrate is negatively charged across the measured pH range (Fig. 2a3). The one-bilayer PEI/GA/PSS/PAH membrane fabricated by subsequently spraying a layer of polycation PAH reduces the negative surface charge with an IEP of pH 5.6 (Fig. 2b3). After the uncharged F127 modifier was further sprayed on to the membrane surface, the IEP increases again to pH 7.07 (Fig. 2b2). The surface of the uncrosslinked PEI/PSS/PAH membrane is positively charged with IEP of pH 9.40 (Fig. 2b1), consistent with our prior work [23,28].

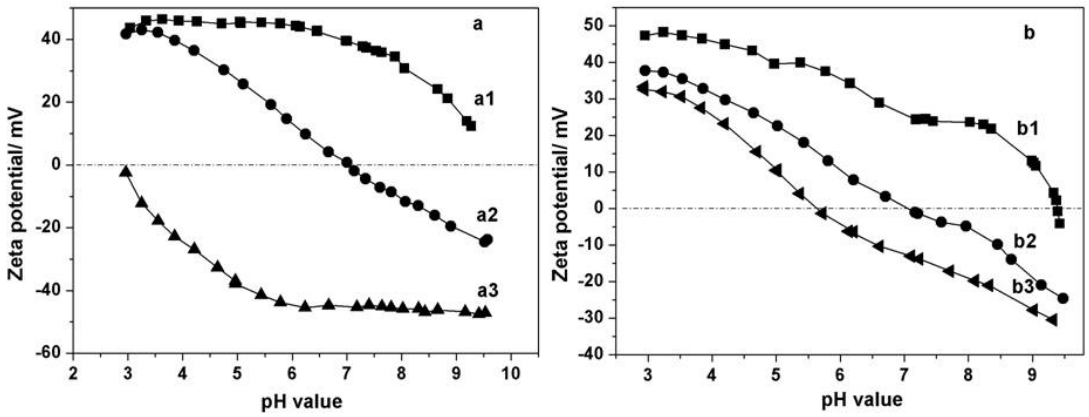

Fig. 2. Zeta potential curves of the various polyelectrolyte membranes. (a1) the PSF substrate sprayed with PEI, (a2) the PSF substrate sprayed with PEI/GA, and (a3) the PSF substrate sprayed with PEI/GA/PSS; (b1) the uncrosslinked PEI/PSS/PAH membrane, (b2) the F127 modified PEI/GA/PSS/PAH/F127, and (b3) the PEI/GA/PSS/PAH membrane.

The significant changes in zeta potential after each spraying step (Fig. 2a,b) illustrates that all the sprayed chemicals (polyelectrolytes, crosslinker, and modifier) were successfully sequentially adsorbed on the substrate surface. As described in Scheme 1, the positively charged PEI layer is firstly deposited on the PSF substrate by electrostatic interaction. After GA was subsequently sprayed on to the substrate, it was partly anchored on the PEI-layer surface by the formation of imine bonds (–C=N–) as mentioned above. Furthermore, the crosslinking reaction also occurred in the inner of the PEI layer. As a result, the positive charge density of the substrate with PEI/GA layer is drastically decreased due to the decrease of the amine groups of PEI layer, and the IEP correspondingly shifts down to pH 7.05 (Fig. 2a2). When the polyanion PSS was further sprayed, a negatively charged PSS layer is formed by the electrostatic interaction with the slightly positively charged PEI/GA layer. The amine groups of the subsequently sprayed PAH layer can react with the unreacted aldehyde groups of the GA to form more imine

bonds (–C=N–). The conversion of the primary amine (pKa=9) into imine (pKa=4) results in the formation of the negatively charged surface of the PEI/GA/PSS/PAH membrane (Fig. 2b3) at neutral pH.

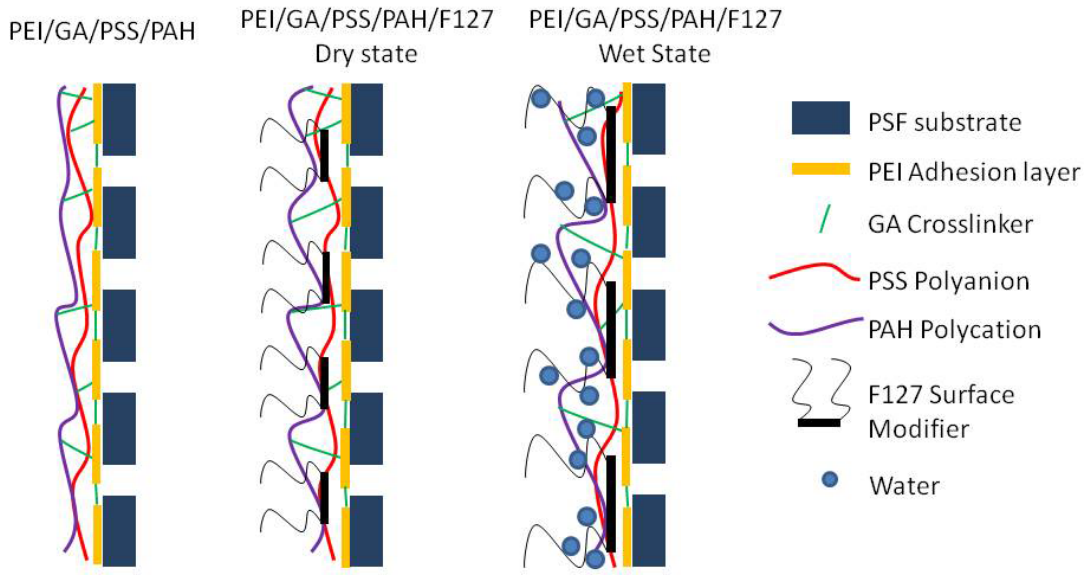

Scheme 1. A schematic illustration of the formation of the crosslinked polyelectrolyte membranes and the structural changes that occur when swollen in water.

Significantly, when the F127 is added, the membrane becomes more positively charged across the full pH range (Fig. 2b2). This suggests that rather than deposition as a surface coating, the central hydrophobic chain within the F127 is penetrating into the LBL structure and driving the positively charged PAH amine groups closer to the surface. The results illustrate that the crosslinker GA and modifier F127 have an important influence on the surface charge properties and structure of the membranes.

Additionally, the F127 modified PEI/GA/PSS/PAH/F127 membrane possesses a lower contact-angle value (55°±3), compared with the unmodified PEI/GA/PSS/PAH membrane

239 (71°±2), indicating that the former is more hydrophilic than the latter due to the presence
240 of hydroxyl (–OH) and ether (–CH_2–O–CH_2–) groups within the F127 polymer.

241 ***3.2. Membrane structure and morphology***

242 Some mesopores (*ca.* 10–20 nm) are clearly visible in the SEM image of the PSF
243 substrate (Fig. 3a, also shown as a larger image in the Supporting Information Fig. S1).
244 The uncrosslinked PEI/PSS/PAH membrane (Fig. 3d and Fig. S4) also appears to show
245 small mesopores. This suggests that very little polyelectrolyte has been deposited on the
246 substrate, which is consistent with the ATR-IR results (Fig. 1). In contrast, the surface of
247 the crosslinked and F127 modified one-bilayer membranes (Fig. 3b and c, also shown as
248 Fig. S2 and S3) become denser and more uniform, indicating a greater surface
249 coverage.The uniform thickness and smooth cross section can be clearly observed after
250 spray LBL in the cross-sectional images (Fig. 4b and c, also shown as Fig. S5 and S6). The
251 thickness of the combined PEI/GA/PSS/PAH layers (Fig. 4b) is *ca.* 50 nm. After F127 was
252 sprayed, the thickness of the combined layers (Fig. 4c) slightly increases to *ca.* 70 nm.

253

254

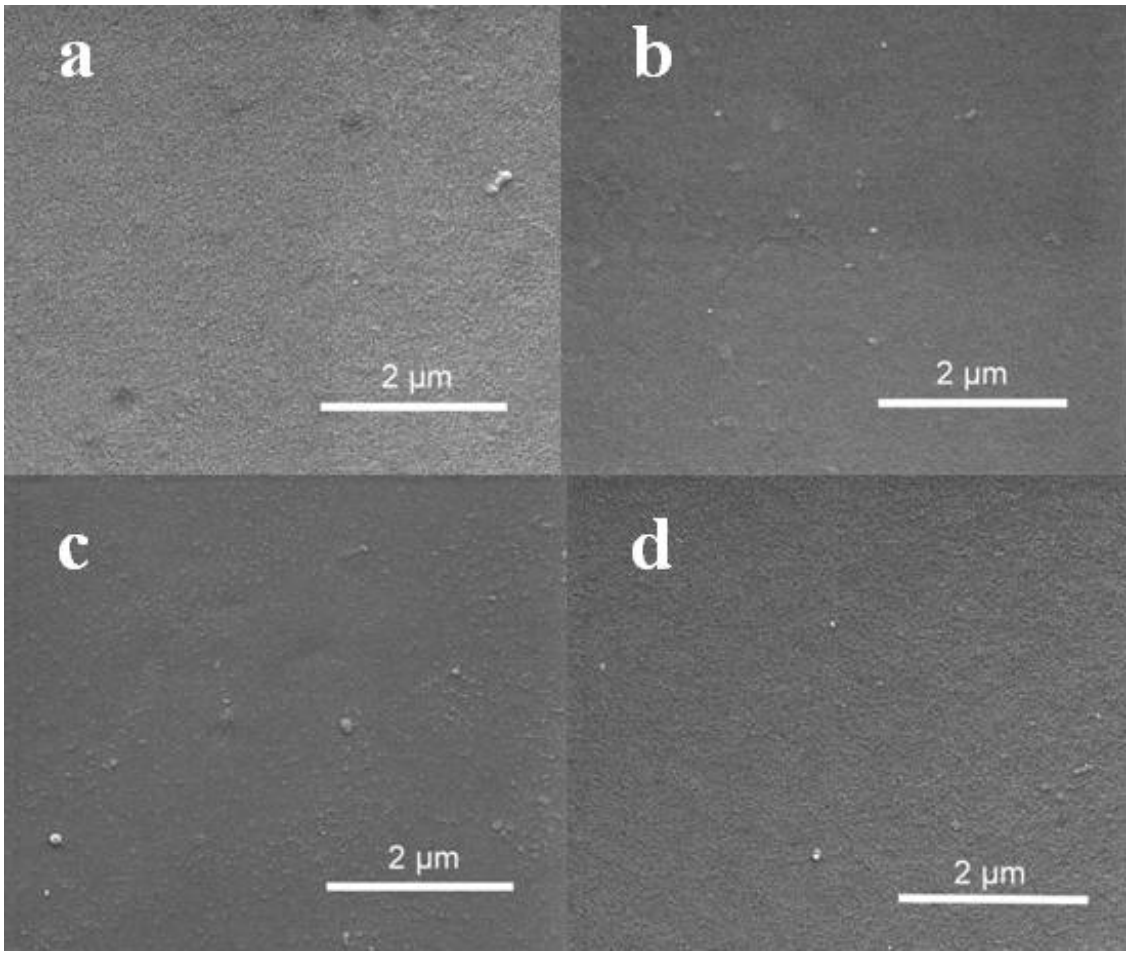

Fig. 3. SEM images of the top surfaces of the (a) PSF substrate; (b) the modified PEI/GA/PSS/PAH/F127 membrane; (c) the unmodified PEI/GA/PSS/PAH membrane and (d) the uncrosslinked PEI/PSS/PAH membrane.

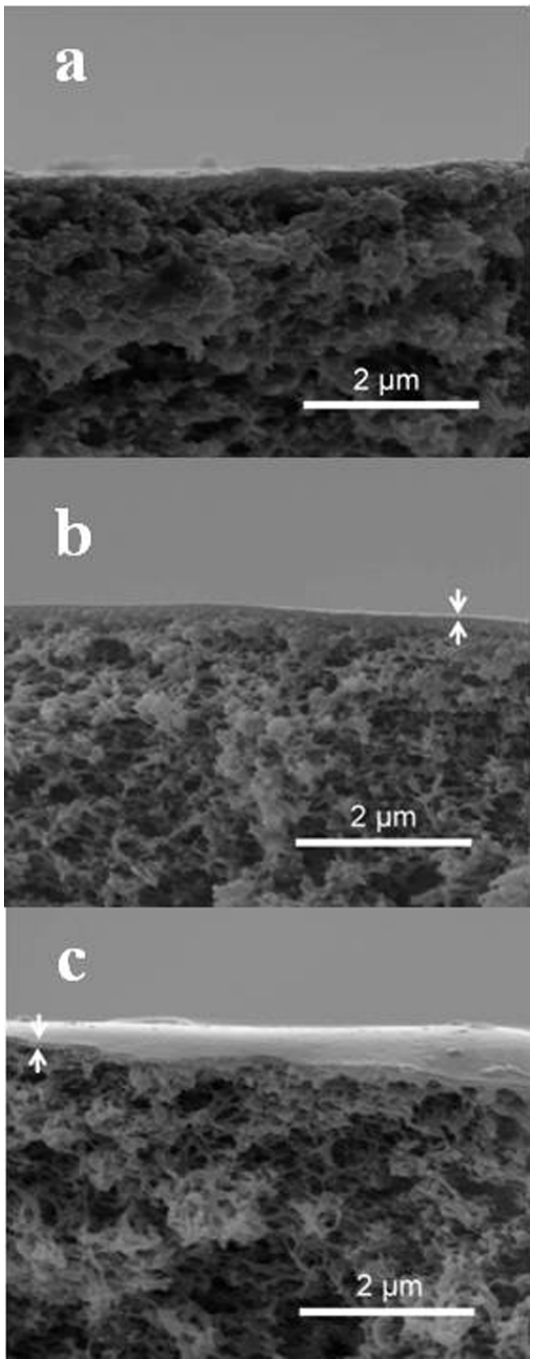

Fig. 4. SEM images of the cross sections of (a) PSF substrate, (b) the unmodified PEI/GA/PSS/PAH membrane, and (c) the F127 modified PEI/GA/PSS/PAH/F127 membrane.

3.3. Membrane separation performance

The F127 modified one-bilayer membrane (PEI/GA/PSS/PAH/F127) shows good separation capability with a 2 g/L NaCl feed solution (pH 5.5 – 6.0) under a crossflow filtration mode (Fig. 5), with an intrinsic membrane permeability of 0.75 L/m^2.h.Bar. The salt rejection and permeate flux are respectively *ca.* 92 % and 11 L/m^{2}h at 1.6 MPa operating pressure. As the operating pressure increases to 4.0 MPa, the permeate flux increases almost linearly to *ca.* 30 L/m^{2}h. Simultaneously, the salt rejection increases to *ca.* 94 %.

The effects of the crosslinker GA, polyelectrolytes PSS/PAH and surface modifier F127 on the separation performance were also investigated at a uniform operating pressure of 2.4 MPa (Table 1). The PEI/GA membrane has low salt rejection (*ca.* 28%) and relatively high permeate flux (*ca.* 35 L/m^{2}h), indicative of both the low charge density of this layer (Figure 2a2) at neutral pH and the potential for defects in this single layer. Moreover, the partial dissolution of the PEI polymer into the feed solution over time made the performance of this membrane unstable. The uncrosslinked PEI/PSS/PAH membrane has higher salt rejection (*ca.* 50 %) indicative of the greater charge density (Figure 2b1) but this is still insufficient to form a useful RO membrane, consistent with our prior work [28]. After the GA is introduced (PEI/GA/PSS/PAH), the salt rejection increases significantly to *ca.* 93 %, but this is accompanied by a drastic loss in permeate flux (*ca.* 3 L/m^{2}h). Interestingly, the subsequent F127 spray step increased the permeate flux to *ca.* 18 L/m^{2}h, while retaining the salt rejection at almost the same level (*ca.* 93 %). In contrast, the commercial SW30HR RO membrane exhibits higher salt rejection (*ca.* 99 %) and permeate flux (*ca.* 22 L/m^{2}h) under the same test conditions. However, a direct comparison to these commercial membranes is inappropriate considering that manufacturers have had the

opportunity to optimize their production for over 40 years; through the use of surfactants, additives and surface coatings [35-37].

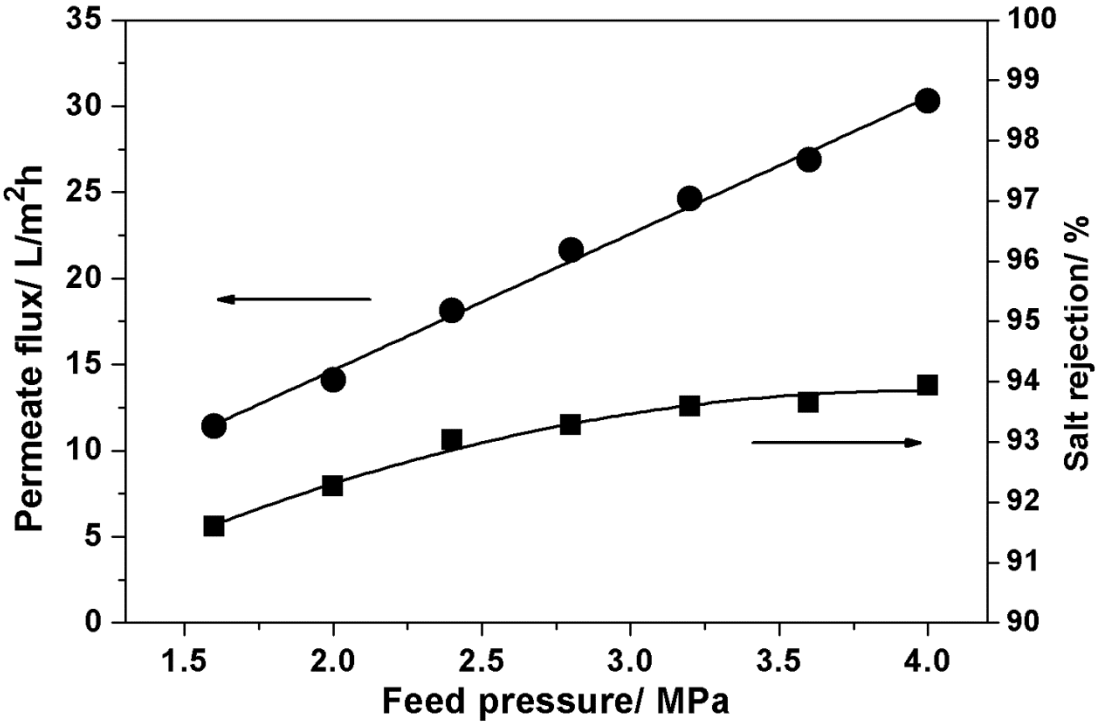

Fig. 5. The salt rejection and permeate flux of the F127 modified one–bilayer PEI/GA/PSS/PAH/F127 membrane versus feed pressures ranging from 1.6 MPa to 4.0 MPa using a 2 g/L NaCl aqueous solution as feed.

The boron rejection of the membranes were tested using 20 mg/L boric acid at 2.4 MPa feed pressure. The results show that both the unmodified PEI/GA/PSS/PAH (*ca.* 88 %) and modified PEI/GA/PSS/PAH/F127 (*ca.* 84 %) membranes exhibit high boron rejection under basic (pH 11) feed conditions where the boric acid is charged [38,39]. Thus, both membranes are sufficiently negatively charged (Fig. 2b) to reject the small borate anion. However, when the pH of the feed solution is adjusted to 4, the PEI/GA/PSS/PAH

membrane still shows high boron rejection (*ca.* 87 %), while the rejection of the PEI/GA/PSS/PAH/F127 membrane falls drastically to *ca.* 33 %. Under these conditions the boric acid is uncharged [38,39]. This confirms the size of the free volume elements are on average, larger than that of a boric acid molecule (~ 2.6 Angstroms[38]) in the F127 modified membrane, so that these uncharged species can readily permeate. Conversely, the free volume elements would appear smaller than 2.6 Angstroms in the PEI/GA/PSS/PAH active layer.

Table 1. Salt rejection and permeate flux of experimental and commercial RO membranes with 2 g/L NaCl feed solution (pH 5.5 – 6.0) at 2.4 MPa feed pressure.

Membrane type	Salt rejection/ %	Permeate flux/ L/m^{2}h
PEI/GA	28 ± 2	35 ± 3
PEI/PSS/PAH	50 ± 3	24 ± 4
PEI/GA/PSS/PAH	93 ± 2	3 ± 1
PEI/GA/PSS/PAH/F127	93 ± 2	18 ± 2
Commercial SW30HR	99.4 ± 0.5	22 ± 2

3.4. Performance stability and protein fouling resistance

The stability of the PEI/GA/PSS/PAH/F127 membrane was evaluated by continuously operation of the membrane for 32 h. The results (Fig. 6) show that the permeate flux was stable at 18.1 ± 0.3 L/m^{2}h, and the salt rejection also fluctuated in a very small range (92.9 ± 0.2 %). This indicates that the membrane possesses excellent separation performance stability.

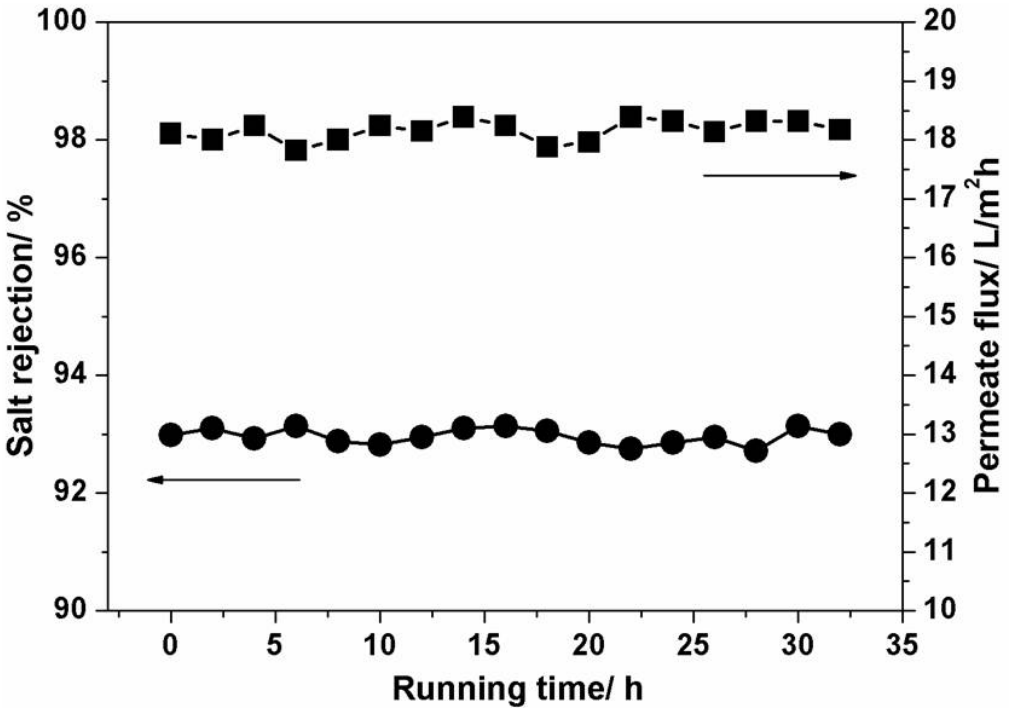

Fig. 6. The separation stability of the modified one-bilayer PEI/GA/PSS/PAH/F127 membrane over 32 h of continuous operation with a 2 g/L NaCl aqueous solution and 2.4 MPa test pressure.

After filtration with 1 g/L BSA solution for 8 h, the normalized permeate flux of the PEI/GA/PSS/PAH/F127 membrane decreased to *ca.* 74 % of the initial value (Fig. 7a). This flux recovered to *ca.* 87 % of this value after flushing with water. Conversely, the permeate flux of the unmodified PEI/GA/PSS/PAH membrane decreased further to *ca.* 68 % and recovered to *ca.* 83 % after flushing (Fig. 7b). After fouling for a further two cycles of 8 h each, the permeate flux of the modified PEI/GA/PSS/PAH/F127 membrane was still 72 % (Fig. 7a), showing little further loss from the first fouling cycle. Conversely, the normalized permeate flux of the unmodified membrane had decreased to *ca.* 61% (Fig. 7b). These results suggest that the F127 surface modification is also favorable for improving

fouling resistance, reflecting the greater hydrophilicity and neutral surface charge of this membrane, which can weaken the interactions with protein foulants [32,34].

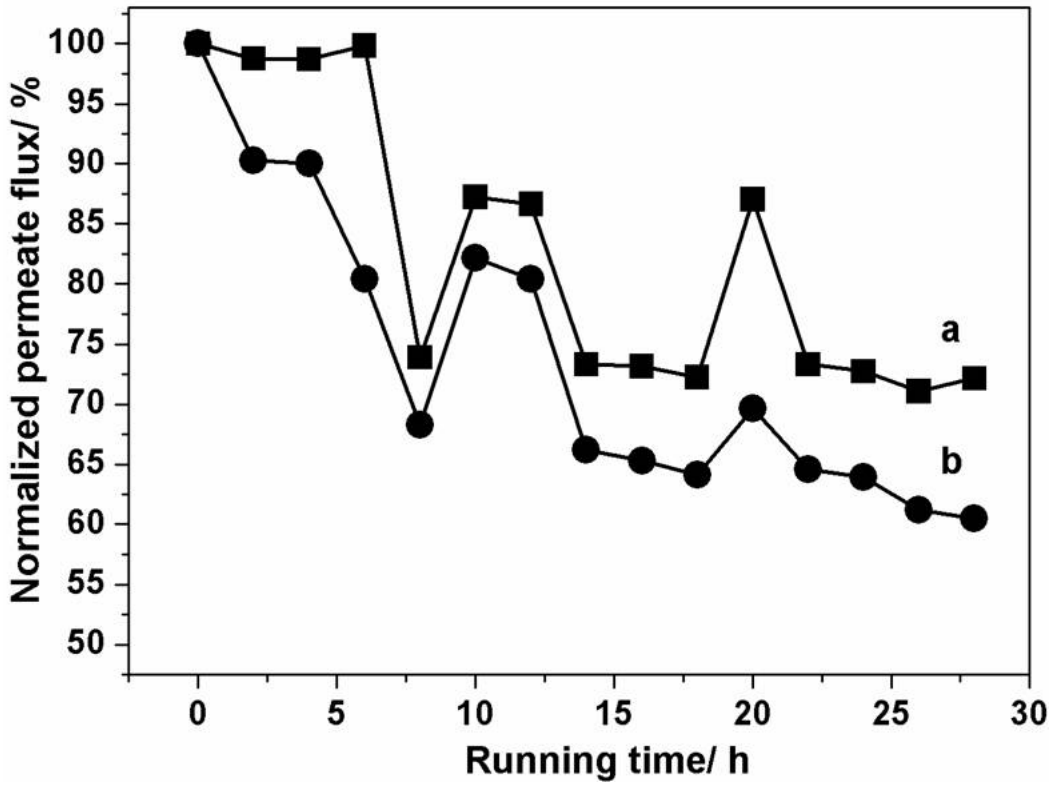

Fig. 7. The normalized permeate fluxes of the (a) modified PEI/GA/PSS/PAH/F127 and (b) unmodified PEI/GA/PSS/PAH membranes in 1 g/L BSA aqueous solution. The initial fluxes of the PEI/GA/PSS/PAH/F127 and PEI/GA/PSS/PAH membranes are 28 L/m^{2}h and 5 L/m^{2}h, respectively.

3.5. The mechanisms of membrane formation and fouling resistance

In this work, GA is deposited as a crosslinker prior to the addition of PAH. This step plays an important role in improving the polyelectrolyte membrane densification and salt rejection. The GA firstly crosslinks with the amine group of the PEI layer by forming imine

bonds (–N=C–) confirmed by the ATR-IR results (Fig. 1). Unreacted aldehyde groups within the GA can further crosslink with the subsequent PAH layer. Relative to our prior work [28], where the 10-bilayer PEI/PSS/PAH membrane was immersed in a GA after the addition of the polyelectrolytes, this makes the PEI layer denser and reduces the defects within the layer (Scheme 1). As a result, this membrane (PEI/GA/PSS/PAH) exhibits a high NaCl rejection (*ca.* 93 %), although it only has one polyelectrolyte bilayer. However, the dense, crosslinked active layer simultaneously decreases the diffusion rate of the permeate and the membrane thus possesses very low permeate flux (*ca.* 3 L/m^2h). The poor rejection of the uncrosslinked one-bilayer PEI/PSS/PAH membrane (*ca.* 50 %) further confirms the importance of the GA crosslinker for improving salt rejection.

After F127 is sprayed onto the surface of the PEI/GA/PSS/PAH membrane, the hydrophobic PPO end partly penetrates into the PAH layer (Scheme 1) by the hydrogen-bond interactions between the ether groups ($–CH_2–O–CH_2–$) of F127 and the unreacted amine groups ($–NH_3^+$) of PAH. Correspondingly, the hydrophilicity of the membrane is improved, with the hydrophilic PEO ends directly exposed to the outside in a brush-like structure [20]. This increased hydrophilicity is confirmed by the contact angle results. When the membrane contacts with water in the desalination process, the F127 expands as it absorbs water. This causes the fractional free volume to increase and the formation of water channels between the F127 chains and the PAH layer (Scheme 1). The formation of the new channels and the improvement of surface hydrophilicity confer the one-bilayer PEI/GA/PSS/PAH/F127 membrane with a higher permeate flux, compared with the unmodified PEI/GA/PSS/PAH membrane.

This hypothesis is confirmed by the boron rejection and zeta potential results (Fig. 2) mentioned above. Poly-borate compounds are negligible in concentration at the boron concentrations used (20 mg/L), and so only boric acid (H_3BO_3) and borate ions ($B(OH)_4^-$)

are present [38]. Boric acid and borate ions have nearly the same Stokes radius (2.6 Å [38]). Under basic conditions (pH=11), the boron is present in the form of borate ions ($B(OH)_4^-$) [38,39]. There is strong charge repulsion between these negatively charged boron ions and the negatively charged surfaces of both the unmodified and the F127 modified one-bilayer membranes (Fig. 2b). The charge repulsion provides both membranes with high boron rejection (*ca.* 88 %). After the pH is adjusted to 4, boron is mainly present in the form of neutral boric acid (H_3BO_3) [38,39]. The unmodified PEI/GA/PSS/PAH membrane still shows a higher boron rejection (*ca.* 87 %) due to the strong densification of the active layer. However, because the active layer of the F127 modified membrane (PEI/GA/PSS/PAH/F127) is swollen and charge repulsion disappears, the boric acid species can readily pass through the active layer. Therefore, the modified PEI/GA/PSS/PAH/F127 membrane possesses a poor boron rejection (*ca.* 33%). The change in boron rejection at different pH values confirms the presence of new water channels in the modified PEI/GA/PSS/PAH/F127 membrane. It is noteworthy that although the surface of the modified membrane (PEI/GA/PSS/PAH/F127) is close to its isoelectric point at neutral pH (Fig. 2b), there is clearly sufficient charge within the underlying layers of the membrane itself to provide strong rejection of charged Na^+ and Cl^- ions, as shown in Table 1.

Moreover, the hydrophobic PPO end of the F127 modifier partly penetrates into the PAH layer (Scheme 1), and the hydrophilic PEO end is directly exposed to the outside, forming a “brush-like” structure on the membrane surface [33]. Such “brush-like” PEO structures have been shown by other workers to provide fouling resistance [40-42]. We believe this is the case for the modified PEI/GA/PSS/PAH/F127 membrane as shown in Fig. 6.

4. Conclusions

A single bilayer polyelectrolyte RO membrane with high salt rejection and permeate flux has been successfully fabricated by a spray-LBL method using PEI as an adhesion promoter, PSS and PAH as polyanion and polycation, GA as a polyelectrolyte crosslinker, and Pluronic F127 as a surface modifier. The GA crosslinker plays an important role in improving the salt rejection by increasing the membrane densification *via* forming imine bonds (–C=N–) within the PEI layer and PEI/PAH interlayer. It restricts the mobility and conformation change of the polyelectrolyte chains, stabilizing the membrane separation performance. The swelling of the F127 in aqueous solution results in the formation of additional free volume for water permeation within the active layer. The deposited F127 also improves the membrane hydrophilicity. These factors confer the membrane with a high permeate flux and improved fouling resistance. Importantly, the membrane can be assembled in a minimum number of processing steps, which will facilitate manufacturing operations at large scale.

Acknowledgments

Qiang Li acknowledges the financial support from the China Scholarship Council (CSC) (No. 201504180033), the National Natural Science Foundation of China (NSFC) (No. 21406041), the special financial fund support from the Public Welfare Project of the Marine Industry (No. 201405009-3) and the Project of Scientific &Technology Support of the 12th Five-year Plan of China (No. 2014BAB06B00) and the support from The University of Melbourne.

418 **References**

419 [1] M.T.M. Pendergast, E.M.V. Hoek, A review of water treatment membrane
420 nanotechnologies, Energy Environ. Sci. 4 (2011) 1946–1971.

421 [2] G.-R. Xu, S.-H. Wang, H.-L. Zhao, S.-B. Wu, J.-M. Xu, L. Li, X.-Y. Liu, Layer-by-
422 layer (LBL) assembly technology as promising strategy for tailoring pressure-driven
423 desalination membranes, J. Membr. Sci. 493 (2015) 428–443.

424 [3] A. Pérez-González, A.M. Urtiaga, R. Ibáñez, I. Ortiz, State of the art and review on the
425 treatment technologies of water reverse osmosis concentrates, Water Res. 46 (2012) 267–
426 283.

427 [4] Q. Li, J. Song, H. Yu, Z. Li, X. Pan, B. Yang, Investigating the microstructures and
428 surface features of seawater RO membranes and the dependencies of fouling resistance
429 performances, Desalination 352 (2014) 109–117.

430 [5] G. Decher, J.D. Hong, J. Schmitt, Buildup of ultrathin multilayer films by a self-
431 assembly process: III. consecutively alternating adsorption of anionic and cationic
432 polyelectrolytes on charged surfaces, Thin Solid Films 210 (1992) 831–835.

433 [6] G. Decher, Fuzzy nanoassemblies: toward layered polymeric multicomposites, Science
434 277 (1997) 1232−1237.

435 [7] J.J. Richardson, M. Björnmalm, F. Caruso, Technology-driven layer-by-layer assembly
436 of nanofilms, Science 348 (2015) 2491–2501.

437 [8] P. Schaaf, J.-C. Voegel, L. Jierry, F. Boulmedais, Spray-assisted polyelectrolyte
438 multilayer buildup: from step-by-step to single-step polyelectrolyte film constructions,
439 Adv. Mater. 24 (2012) 1001–1016.

[9] R. Blell, X. Lin, T. Lindstr□m, M. Ankerfors, M. Pauly, O. Felix, G. Decher, Generating in-plane orientational order in multilayer films prepared by spray-assisted layer-by-layer assembly, ACS Nano 11 (2017) 84−94.

[10] A. Gopalakrishnan, M.L. Mathew, J. Chandran, J. Winglee, A.R. Badireddy, M. Wiesner, C.T. Aravindakumar, U.K. Aravind, Sustainable polyelectrolyte multilayer surfaces: possible matrix for salt/dye separation, *ACS Appl. Mater. Interfaces,* 7 (2015) 3699−3707.

[11] J. Borges, J.F. Mano, Molecular interactions driving the layer-by-layer assembly of multilayers, Chem.Rev. 114 (2014) 8883–8942.

[12] H. Zhen, T. Wang, R. Jia, B. Su, C. Gao, Preparation and performance of antibacterial layer-by-layer polyelectrolyte nanofiltration membranes based on metal–ligand coordination interactions, RSC Adv. 5 (2015) 86784–86794.

[13] X. Zhang, H. Chen, H. Zhang, Layer-by-layer assembly: From conventional to unconventional methods, Chem. Commun. (2007) 1395–1405.

[14] L.Y. Ng, A.W. Mohammad, C.Y. Yin, A review on nanofiltration membrane fabrication and modification using polyelectrolytes: Effective ways to develop membrane selective barriers and rejection capability, Adv. Colloid Interface Sci. 197–198 (2013) 85–107.

[15] B. Su, T. Wang, Z. Wang, X. Gao, C. Gao, Preparation and performance of dynamic layer-by-layer PDADMAC/PSS nanofiltration membrane, J. Membr. Sci. 423 (2012) 324–331.

461 [16] J. Meier-Haack, W. Lenk, D. Lehmann, K. Lunkwitz, Pervaporation separation of
462 water/alcohol mixtures using composite membranes based on polyelectrolyte multilayer
463 assemblies, J. Membr. Sci. 184 (2001) 233−243.

464 [17] C. Qiu, S. Qi, C.Y. Tang, Synthesis of high flux forward osmosis membranes by
465 chemically crosslinked layer-by-layer polyelectrolytes, J. Membr. Sci. 381 (2011) 74–80.

466 [18] D. Saeki, M. Imanishi, Y. Ohmukai, T. Maruyama, H. Matsuyama, Stabilization of
467 layer-by-layer assembled nanofiltration membranes by crosslinking via amide bond
468 formation and siloxane bond formation, J. Membr. Sci. 447 (2013), 128–133.

469 [19] J. Grooth, R. Oborný, J. Potreck, K. Nijmeijer, W.M. Vos, The role of ionic strength
470 and odd–even effects on the properties of polyelectrolyte multilayer nanofiltration
471 membranes, J. Membr. Sci. 475 (2015) 311–319.

472 [20] T. Wang, J. Lu, L. Mao， Z. Wang, Electric field assisted layer-by-layer assembly of
473 grapheme oxide containing nanofiltration membrane, J. Membr. Sci. 515 (2016) 125–133.

474 [21] J. Park, J. Park, S.H. Kim, J. Cho, J. Bang, Desalination membranes from pH-
475 controlled and thermally-crosslinked layer-by-layer assembled multilayers, J. Mater.
476 Chem. 20 (2010) 2085–2091.

477 [22] P.H.H. Duong, J. Zuo, T.-S. Chung, Highly crosslinked layer-by-layer polyelec-
478 trolyte FO membranes: Understanding effects of salt concentration and deposition time on
479 FO performance, J. Membr. Sci. 427 (2013) 411–421.

480 [23] K.L. Cho, H. Lomas, A.J. Hill, F. Caruso, S.E. Kentish, Spray assembled, cross-linked
481 polyelectrolyte multilayer membranes for salt removal, Langmuir 30 (2014) 8784−8790.

[24] H. Tang, G. Zhang, S. Ji, Rapid assembly of polyelectrolyte multilayer membranes using an automatic spray system, AIChE J. 59 (2013) 250–257.

[25] A. Toutianoush, L. Krasemann, B. Tieke, Polyelectrolyte multilayer membranes for pervaporation separation of alcohol/water mixtures, Colloids Surfaces A Physicochem. Eng. Asp. 198 (2002) 881–889.

[26] J.B. Schlenoff, S.T. Dubas, T. Farhat, Sprayed polyelectrolyte multilayers, Langmuir 16 (2000) 9968−9969.

[27] H. Tang, S. Ji, L. Gong, H. Guo, G. Zhang, Tubular ceramic-based multilayer separation membranes using spray layer-by-layer assembly, Polym. Chem. 4 (2013) 5621–5628.

[28] K.L. Cho, A. J. Hill, F. Caruso, S.E. Kentish, Chlorine resistant glutaraldehyde crosslinked polyelectrolyte multilayer membranes for desalination, Adv. Mater. 27 (2015) 2791–2796.

[29] Y.-N. Kwon, S. Hong, H. Choi, T. Tak, Surface modification of a polyamide reverse osmosis membrane for chlorine resistance improvement, J. Membr. Sci. 415 (2012) 192–198.

[30] W. Choi, J. Choi, J. Bang, J.-H. Lee, Layer-by-layer assembly of graphene oxide nanosheets on polyamide membranes for durable reverse-osmosis applications, ACS Appl. Mater. Interfaces 5 (2013) 12510−12519.

[31] Y. Jin, Y. Hua, P. Zhang, Y. Yun, P. Zhang, C. Li, Preparation and characterization of poly(vinylidene fluoride) ultrafiltration membrane with organic and inorganic porogens, Desalination 336 (2014) 1–7.

504 [32] Y. Zhang, Y. Su, W. Chen, J. Peng, Y. Dong, Z. Jiang, H. Liu, Appearance of
505 poly(ethylene oxide) segments in the polyamide layer for antifouling nanofiltration
506 membranes, J. Membr. Sci. 382 (2011) 300–307.

507 [33] C.H. Loh, R. Wang, L. Shi, A.G. Fane, Fabrication of high performance
508 polyethersulfone UF hollow fiber membranes using amphiphilic pluronic block
509 copolymers as pore-forming additives, J. Membr. Sci. 380 (2011) 114–123.

510 [34] W. Falath, A. Sabir, K.I. Jacob, Novel reverse osmosis membranes composed of
511 modified PVA/gum arabic conjugates: Biofouling mitigation and chlorine resistance
512 enhancement, Carbohyd. Polym. 155 (2017) 28–39.

513 [35] W.J. Lau, A.F. Ismail, N. Misdan, M.A. Kassim, A recent progress in thin film
514 composite membrane: A review, Desalination, 287 (2012) 190-199.

515 [36] C.Y. Tang, Y.-N. Kwon, J.O. Leckie, Probing the nano- and micro-scales of reverse
516 osmosis membranes—A comprehensive characterization of physiochemical properties of
517 uncoated and coated membranes by XPS, TEM, ATR-FTIR, and streaming potential
518 measurements, Journal of Membrane Science, 287 (2007) 146-156.

519 [37] A. Widjaya, T. Hoang, G.W. Stevens, S.E. Kentish, A comparison of commercial
520 reverse osmosis membrane characteristics and performance under alginate fouling
521 conditions, Separation and Purification Technology, 89 (2012) 270-281.

522 [38] K. Kezia, J. Lee, A. J. Hill, S.E. Kentish, Convective transport of boron through a
523 brackish water reverse osmosis membrane, J. Membr. Sci. 445 (2013)160–169.

524 [39] D. David, H. Ingemar, Research paper: Ionic medium effects in sea water—a
525 comparison of acidity constants of carbonic acid and boric acid in sodium chloride and
526 synthetic sea water, Mar. Chem. 1 (1973) 137–149.

527 [40] G. Kaltali, H. Kalipcilar, P.Z. Culfaz-Emecen, Effect of three different PEO-
528 containing additives on the fouling behavior of PES-based ultrafiltration membranes, Sep.
529 Purificat. Technol. 150 (2015) 21–28

530 [41] A. Asatekin, S. Kang, M. Elimelech, A.M. Mayes, Anti-fouling ultrafiltration
531 membranes containing polyacrylonitrile-graft-poly (ethylene oxide) comb copolymer
532 additives, J. Membr. Sci. 298 (2007) 136–146.

533 [42] F. Liu, C.-H. Du, B.-K. Zhu, Y.-Y. Xu, Surface immobilization of polymer brushes
534 onto porous poly(vinylidene fluoride) membrane by electron beam to improve the
535 hydrophilicity and fouling resistance, Polymer 48 (2007) 2910–2918.

536

537

538

Supporting Information

Spray Assisted Layer-by-Layer Assembled One-Bilayer Polyelectrolyte Reverse Osmosis Membranes

Qiang Li,[a] George Q. Chen,[b] Liang Liu,[b] and Sandra E. Kentish*[b]

[a] The Institute of Seawater Desalination and Multipurpose Utilization, SOA (Tianjin), Tianjin 300192, China

[b] Department of Chemical Engineering, The University of Melbourne, VIC 3010, Australia

*Corresponding Author E-mail: sandraek@unimelb.edu.au (S. E. Kentish).

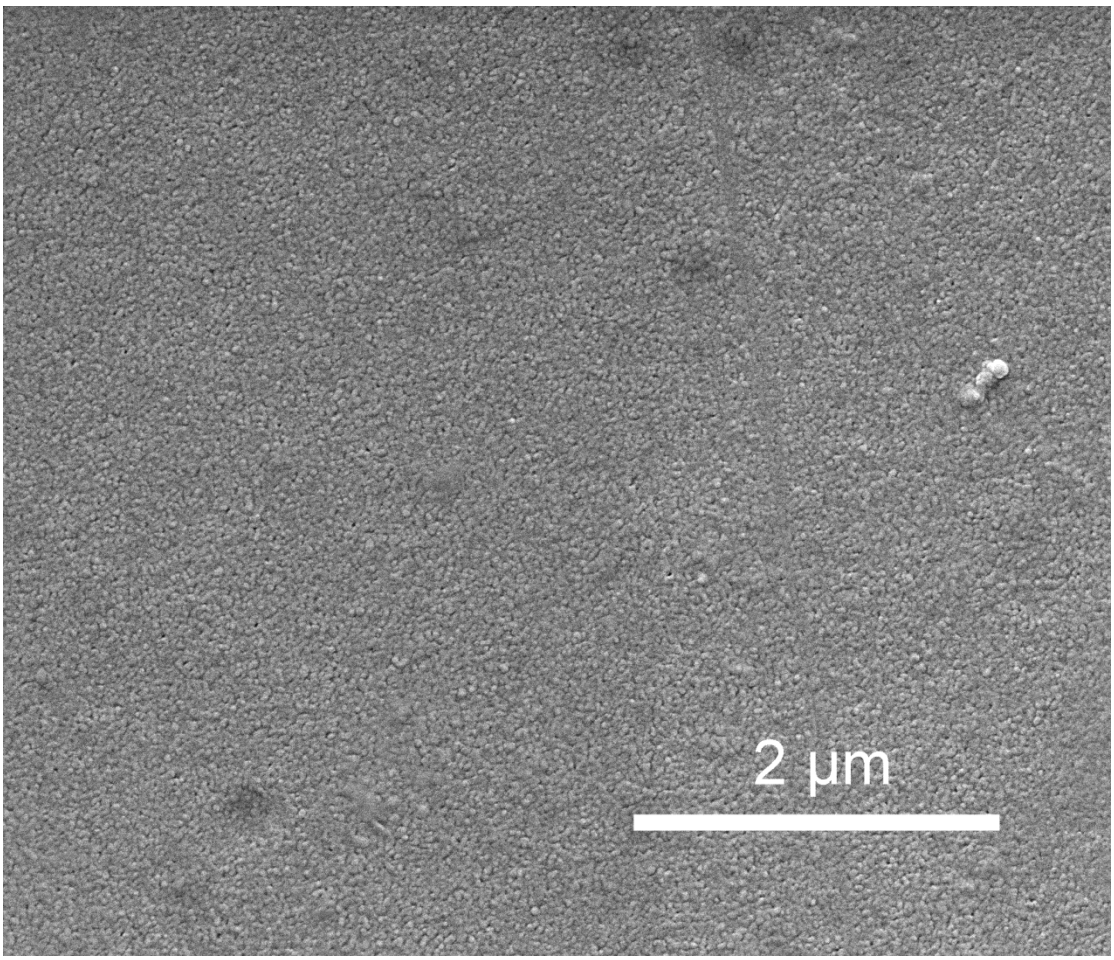

Fig. S1. SEM images of the top surface of the PSF substrate.

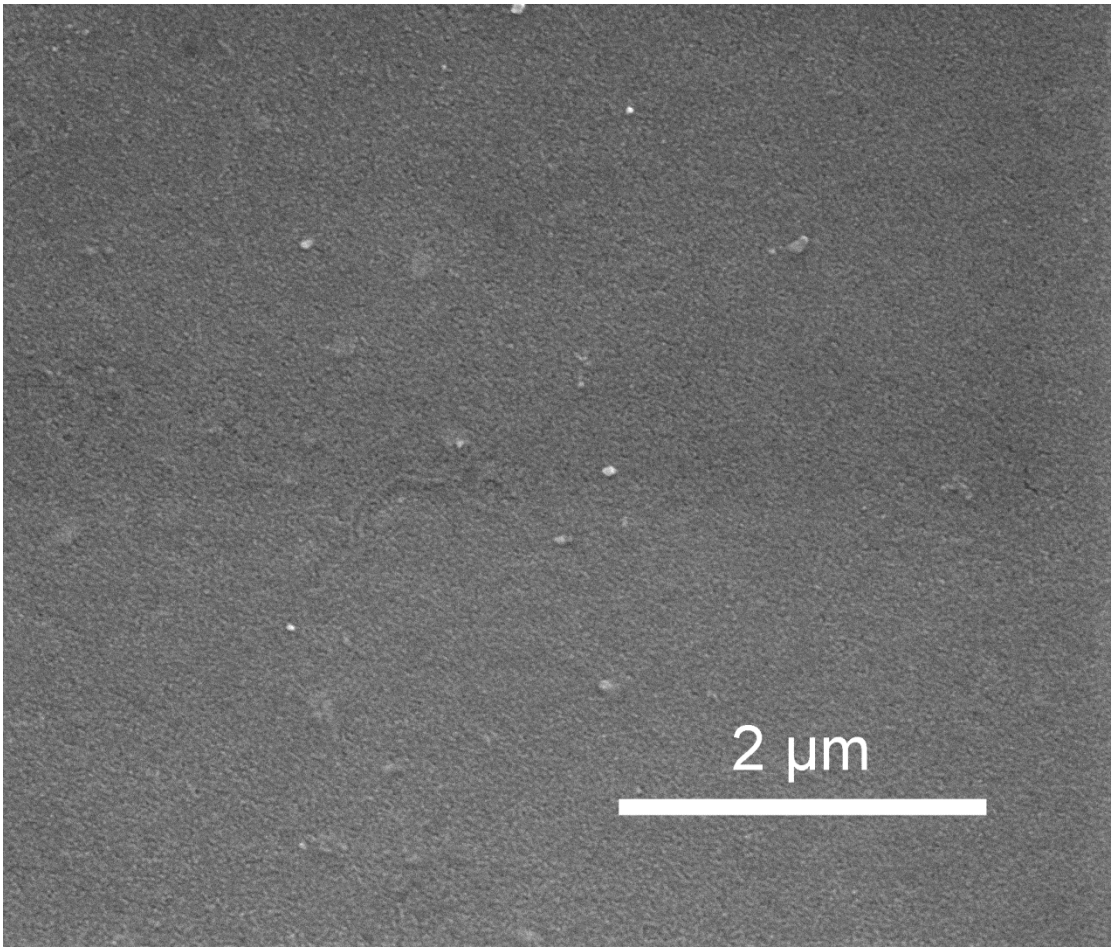

Fig. S2. SEM image of the top surface of the modified PEI/GA/PSS/PAH/F127 membrane.

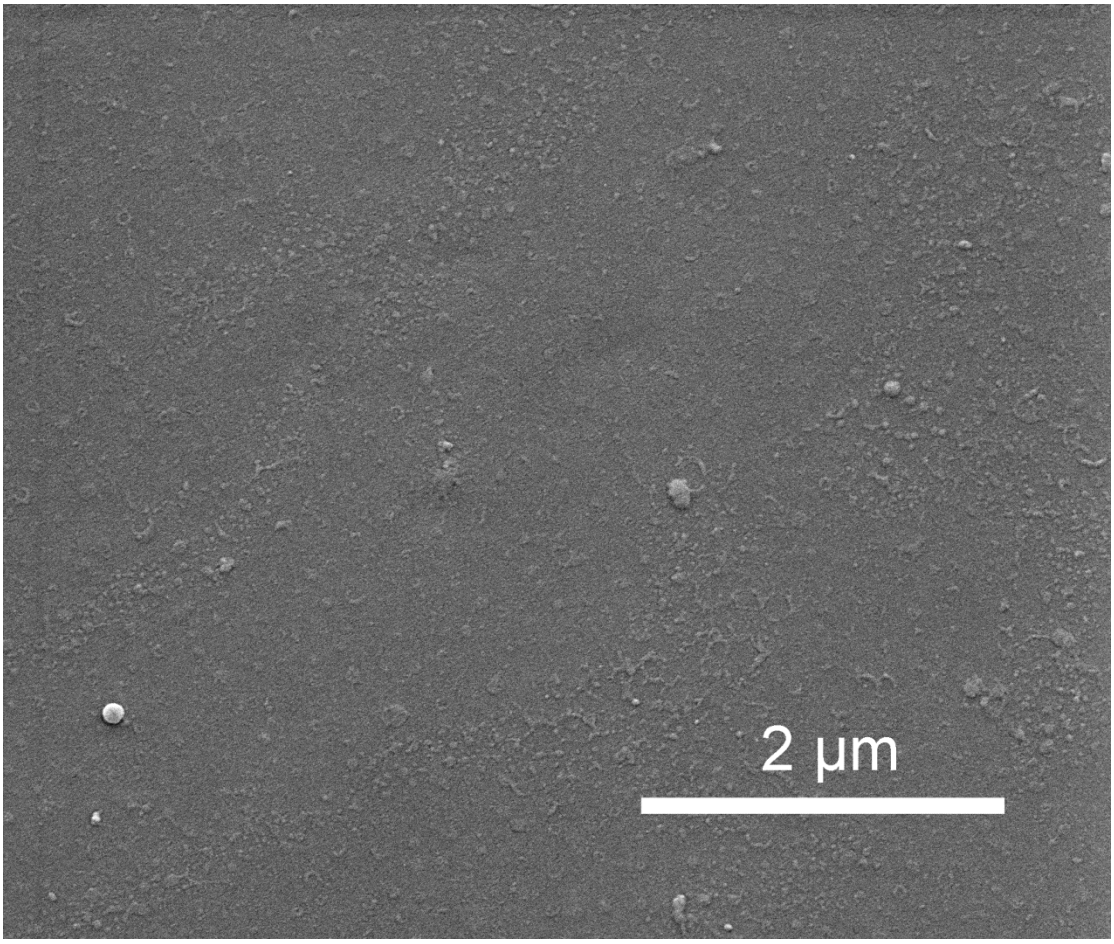

Fig. S3. SEM image of the top surface of the unmodified PEI/GA/PSS/PAH membrane

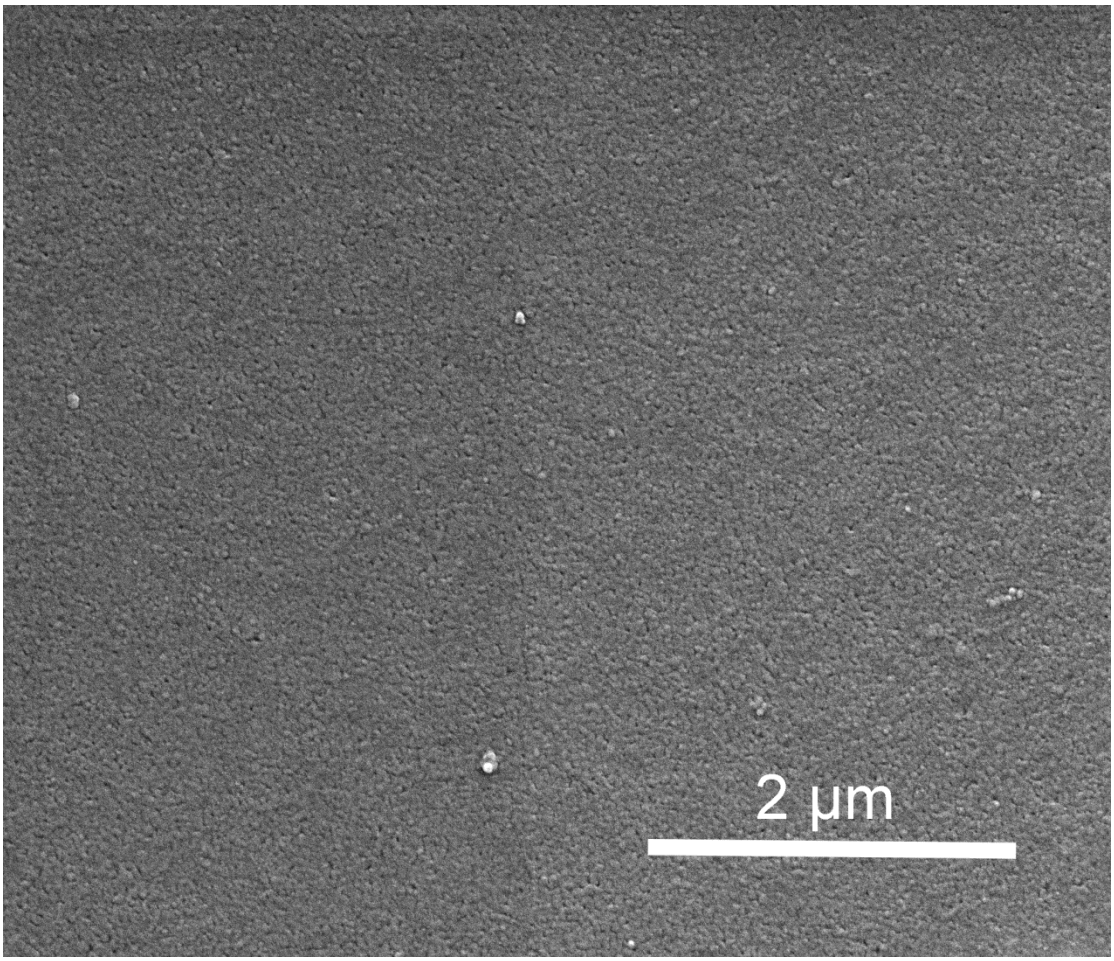

Fig. S4. SEM images of the top surfaces of the uncrosslinked PEI/PSS/PAH membrane.

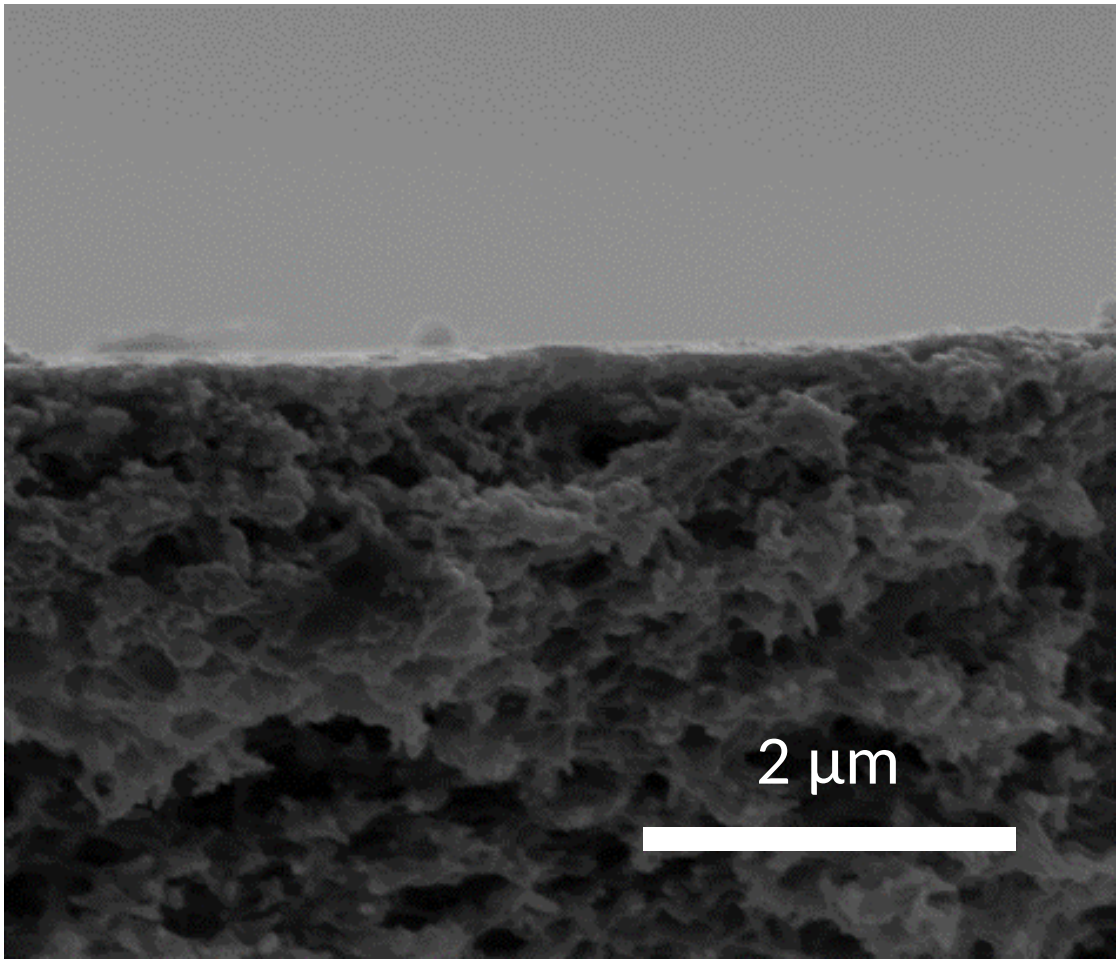

Fig. S5. SEM image of the cross section of the PSF substrate.

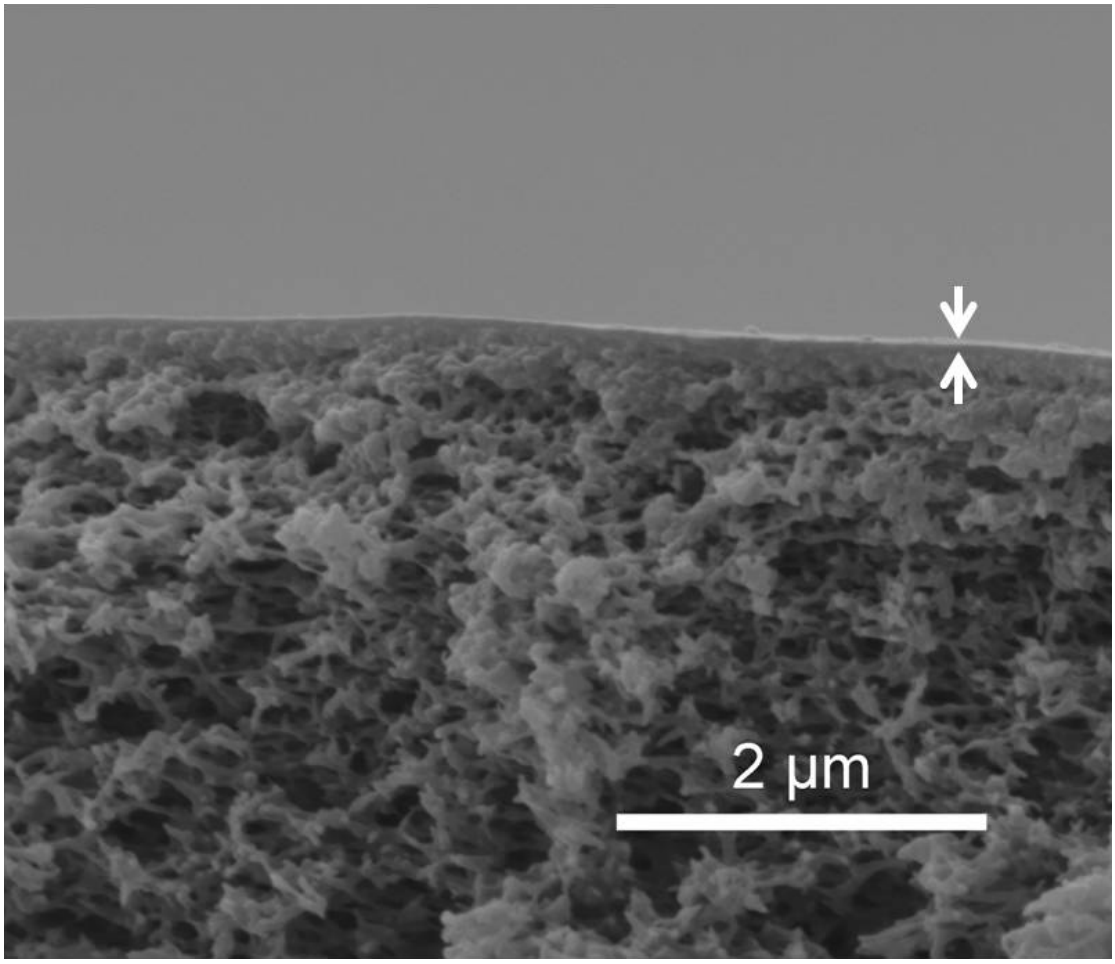

Fig. S6. SEM image of the cross section of the unmodified PEI/GA/PSS/PAH membrane.

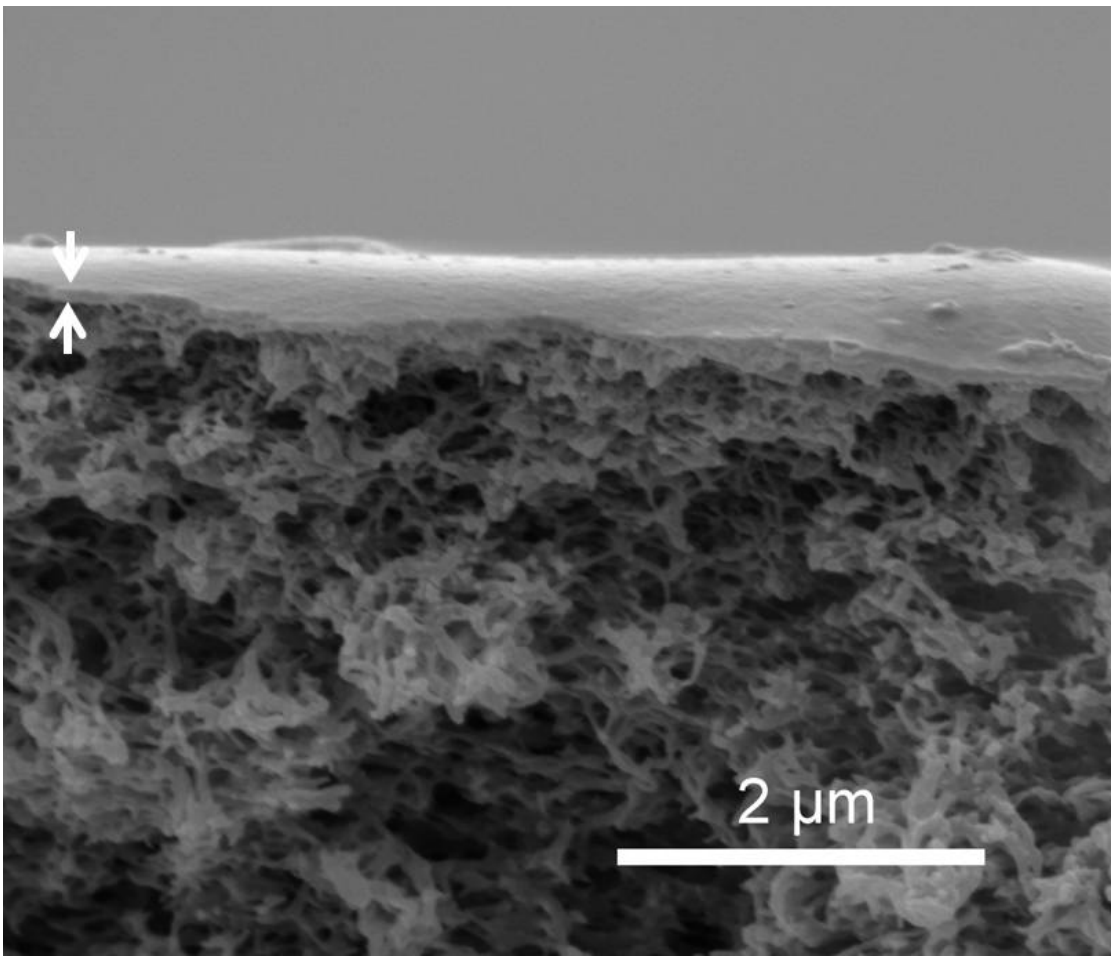

Fig. S7. SEM image of the cross section of the F127 modified PEI/GA/PSS/PAH/F127 membrane.